The targeted heating and current drive applications for the ITER electron cyclotron system

Cite as: Phys. Plasmas **22**, 021808 (2015); https://doi.org/10.1063/1.4908598
Submitted: 09 August 2014 . Accepted: 03 February 2015 . Published Online: 20 February 2015

M. Henderson, G. Saibene, C. Darbos, D. Farina, L. Figini, M. Gagliardi, F. Gandini, T. Gassmann, G. Hanson, A. Loarte, T. Omori, E. Poli, D. Purohit, and K. Takahashi

The targeted heating and current drive applications for the ITER electron cyclotron system

M. Henderson,[1] G. Saibene,[2] C. Darbos,[1] D. Farina,[3] L. Figini,[3] M. Gagliardi,[2] F. Gandini,[1] T. Gassmann,[1] G. Hanson,[4] A. Loarte,[1] T. Omori,[1] E. Poli,[5] D. Purohit,[1] and K. Takahashi[6]
[1]*ITER Organization, Route de Vinon-sur-Verdon, CS 90 046, 13067 St. Paul Lez Durance Cedex, France*
[2]*Fusion for Energy, Josep Pla 2, Barcelona 08019, Spain*
[3]*Istituto di Fisica del Plasma CNR, 20125 Milano, Italy*
[4]*US ITER Project Office, ORNL, 1055 Commerce Park, PO Box 2008, Oak Ridge, Tennessee 37831, USA*
[5]*Max-Planck-Institut für Plasmaphysik, D-85748 Garching, Germany*
[6]*Japan Atomic Energy Agency (JAEA), Naka, Ibaraki 311-0193, Japan*

(Received 9 August 2014; accepted 3 February 2015; published online 20 February 2015)

A 24 MW Electron Cyclotron (EC) system operating at 170 GHz and 3600 s pulse length is to be installed on ITER. The EC plant shall deliver 20 MW of this power to the plasma for Heating and Current Drive (H&CD) applications. The EC system is designed for plasma initiation, central heating, current drive, current profile tailoring, and Magneto-hydrodynamic control (in particular, sawteeth and Neo-classical Tearing Mode) in the flat-top phase of the plasma. A preliminary design review was performed in 2012, which identified a need for extended application of the EC system to the plasma ramp-up, flattop, and ramp down phases of ITER plasma pulse. The various functionalities are prioritized based on those applications, which can be uniquely addressed with the EC system in contrast to other H&CD systems. An initial attempt has been developed at prioritizing the allocated H&CD applications for the three scenarios envisioned: ELMy H-mode (15 MA), Hybrid (∼12 MA), and Advanced (∼9 MA) scenarios. This leads to the finalization of the design requirements for the EC sub-systems. [http://dx.doi.org/10.1063/1.4908598]

I. INTRODUCTION

The ITER plasmas are to be heated by four auxiliary systems: Neutral Beam (NB), Ion Cyclotron (IC), Electron Cyclotron (EC), and Lower Hybrid (LH). The first three are to be installed prior to DT operation with the relative powers listed in Table I. Note that the LH system is planned for a future power upgrade during the DT phase. The combination of the four heating systems provides a versatile set of actuators for the control of the plasma temperature and current profiles as well as plasma instabilities.[1] In addition, ITER will explore different plasma scenarios: ELMy (Edge Localized Mode) H-mode, Advanced and Hybrid; that need varying functionalities from each of the Heating and Current Drive (H&CD) systems.

Also included in Table I are the functionalities assumed for each of the H&CD systems. Note that the partitioning does not necessarily imply a given H&CD system has sufficient power or flexibility to achieve the desired function, but that the given system is better adapted as compared to the other systems to achieve that function. The EC system has been optimized aiming at maximizing the H&CD functional capabilities based on the envisioned applications for each of the three plasma scenarios.[2,3] The optimization concentrated on the unique features offered by an EC H&CD system, avoiding unnecessary redundancy of functions achieved by the other heating systems and balancing against technological risks. Note that each heating system has inherent strengths (as well as limitations), with the EC system offering extremely localized heating and/or driven current with the deposition controllable from external actuators (steerable mirrors), a required feature for the control of the current profile and Magneto-hydrodynamic (MHD) instabilities: Sawteeth oscillations and Neo-classical Tearing Modes (NTMs). In addition, complete power absorption occurs at moderate plasma temperatures and densities, rending the system applicable during the ramp-up and ramp-down phases of ITER plasma pulses. The capacity for heating at resonant (fundamental O1 and second harmonic X2) and intermediate toroidal magnetic fields (B_0) has been demonstrated over much of the range between 2.5 T and 5.3 T.[4]

The aim of this paper is to summarize the capabilities of the EC system[5] for the functions outlined in Table I and then to describe how the EC system has been adapted to best achieve these functions, while balancing the integration and technical challenges.[6] Section II provides brief description of the plasma scenarios and associated operating conditions (fueling, plasma parameters, magnetic field, etc.) envisioned for ITER. The following chapter describes a generic plasma pulse, dividing the pulse into four sequences: plasma initiation, ramp-up, flat-top, and ramp-down. In each period, the applicable EC functions are described, which then establish the design basis for the various sub-systems comprising the EC plant. A brief description of the EC plant is then provided in Sec. IV followed by the Next Steps (Sec. V).

II. PLASMA SCENARIOS AND EC COMMISSIONING PHASES

The commissioning of the EC system strongly depends on the objectives for plasma heating and current drive in the different phases of the ITER tokamak operations. The ITER plasma development advances in phases from an initial short duration discharge for the first plasma, through a

TABLE I. The planned and potential H&CD power levels for the four heating systems and the correlated functional strengths of each of these systems (in addition to the common primary function of bulk heating).

	Injected power			Functional strengths	
System	1st plasma	1st campaign	Potential upgrade	Primary	Secondary
NB	0	33 MW	50 MW	Bulk current drive, plasma rotation	Current profile tailoring, ion heating
IC	0	20 MW	40 MW	Ion heating, impurity control	MHD control
EC	6.7 MW	20 MW	40 MW	Current profile tailoring, MHD control, impurity control	Bulk current drive
LH	0	0	40 MW	Bulk current drive	

non-activation phase and eventually leading to full D-T operation. The aim of this chapter is to review these phases and how they link to the H&CD objectives on the EC system and its corresponding commissioning plan.

The ITER commissioning will be performed in two steps prior to proceeding to D and DT operation.[7] The first step is achieving an initial plasma with limited injected power ($\leq$6.7 MW) and minimum pulse length of 100 ms. The second step uses gas fueling (H or He) that avoids activation during the machine qualification. The EC system plays a critical role in all three of these phases, as described in Subsections II A–II C.

The EC system itself has a phased commissioning program. All critical components will undergo prototype testing for longevity and high power transmission. Once a design has been validated, the manufacturing starts and is concluded with an acceptance test program that demonstrates long pulse high power operation. The various components are delivered to ITER, assembled and follow an on-site acceptance to ensure equivalent operation as achieved at the factory. The EC commissioning will progress in parallel with the tokamak commissioning, with the EC system delivered power and pulse length extended as the plasma pulse and power needs increase. Note that the key component for in-situ commissioning will be the launchers, which can only be tested for single beam transmission prior to installation on the tokamak.

A. First plasma

The initial commissioning of the primary tokamak systems (cryogenics, magnets, vacuum vessel, etc) will conclude with a first plasma, which will be a short pulse ($\geq$0.1 s), low plasma current ($\geq$0.1 MA), low temperature, and low density breakdown. The EC system will be required for this first commissioning phase. The initial "spark" to generate the plasma breakdown will be obtained by injecting second harmonic (X2) EC into the empty plasma chamber. An envisioned 6.7 MW injected power will be available for the initial breakdown, which implies eight 1 MW sources (or gyrotrons) and associated power supplies (PS), transmission lines (TLs), and one of the four upper EC launchers.

These EC sub-systems will be commissioned prior to operation to ensure correct characterization of transmitted power and polarization as needed for the initial breakdown and burnthrough. Note that commissioning requirements for the first plasma are relatively relaxed ($\leq$100 ms). However, the 8 PS-Gyrotron-TL combinations are to be fully calibrated and capable of extended pulse lengths in preparation for the next operating phase.

B. Pre DT operation

The non-activated phase allows qualifying of the tokamak and its many functions (in particular, associated with nuclear confinement), development of the plasma scenarios and plasma control (including critical systems such as ELM coils) prior to its activation. The plasma operation will start with L-mode operation at half field, then extending the performance to H-mode operation, exploring the power thresholds for L to H-mode transition. This is a key phase for the H&CD systems, allowing commissioning of these systems and verification of the total power necessary to achieve the H-mode when extrapolating to full field and DT fuelling.

The envisioned plasma scenarios during the non-activated phase are briefly characterized in Table II, which include typical plasma pulse lengths, number of pulses, and envisioned NTM activity. These values are used to estimate the number of EC pulses and launcher steering mirror rotation cycles, which are used as engineering inputs for estimating the fatigue cycles to the EC launchers, transmission lines, and gyrotrons.

The entire EC system will be installed and commissioned prior to this 1st operating campaign. The commissioning includes calibration of the injected power (up to but excluding the launchers), beam polarization, EC instrumentation and control (I&C) system, nuclear safety functions, occupational safety functions, investment protection functions, etc. In addition, alignment of the launcher steering mirrors will be performed at short pulse injection into an empty torus (target temporarily installed on inner column) and/or use of lasers aligned at the launcher entries to simulate beam paths.

Once plasma operation begins, a series of commissioning pulses are used to cross check the beam alignment and polarization. The injected EC power and pulse length will be increased in a stepwise process, monitoring the behavior of the stray radiation, mirror loading, behavior of the diamond windows, steering mechanism (SM), etc. This process will be performed in parallel with the extension of the plasma pulse length and plasma current. Once correct behavior of a given beam line is demonstrated, that beam line will be ready for service for H&CD applications.

Note that injection of EC power for any new H&CD application will necessitate a commissioning phase to ensure that the EC system is performing the desired function

TABLE II. List and description of plasma pulse types assumed for the pre-DT operating phase. A total of 20 000 pulses are assumed.

Plasma species	I_P and B_T (%)	Mode	q_{min}	τ_{plasma} (flat top) (s)	No. of pulses	NTMs
H/He/D	~50	L-mode	≤1	300	8000	None
He/D	~50	H-mode	≤1	300	6000	q = 3/2, 2
H/He/D	75–100	L-mode	≤1	100	4000	q = 3/2, 2
D	75–100	H-mode	≤1	50	2000	q = 3/2, 2

according to theoretical or modeling expectations. This includes validation of the associated control algorithms.

The non-activated scenarios place the greatest burden on the H&CD systems, as there is no alpha particle heating and the H/He plasmas need more auxiliary power to reach the L-to-H-mode threshold than DT plasmas. In addition, the tokamak will be operating a wide range of densities and at specific toroidal magnetic field values occurring in a range of $2.6\,T < B_0 < 5.3\,T$, further challenging accessibility for all three heating systems. The flexibility of the EC launchers ensures a large range of deposition across the plasma cross section not only at the nominal toroidal magnetic field ($B_0 = 5.3\,T$) corresponding to O1 heating and half field with X2 but also over a large range of intermediate fields.[4] This offers the flexibility of utilizing the EC system for central heating (inside the normalized radius of $\rho < 0.5$) in the range of $2.6\,T < B_0 < 3.2\,T$ and $4.1 < B_0 < 5.3\,T$. The EC system is applicable over an even larger toroidal magnetic field range for assisting in the L-mode to H-mode transition (inside $\rho < 0.85$) $2.6\,T < B_0 < 3.6\,T$ and $4.0 < B_0 < 5.3\,T$. This will be instrumental in determining the H-mode power threshold at nominal field, which will be extrapolated from the stepwise increase of the toroidal magnetic field during the non-active phase of operation and validate the heating power for the L to H-mode transition at 5.3 T.

Prior to either D or DT operation will be the last moment to assess the technical state of the in-vessel components prior to their activation. Potential inspection and revision of components will be considered, while repair operations can still be "hands-on" (note that the launchers will be beryllium contaminated). Once either D or DT operation is initiated, the in-vessel components can only be repaired in the hot cell by remote handling operations.

C. D and DT operation

The ITER research plan includes a short period of D operation, which permits final commissioning of the system with H-mode operation at nominal fields prior to DT operation. This ensures safe operation of the nuclear facility prior to full activation. The D operation is limited in time duration as the tokamak and in-vessel components will be quickly activated, and there will be considerable scientific and political pressure to demonstrate DT operation. The D operation at nominal field will likely be the most challenging on the EC system, full field operation will utilize a maximum amount of injected power, with careful power management between central heating versus control of MHD activity. Note that the DT operation will include alpha particle heating relaxing the demand on the H&CD systems. The active phase of ITER will start as soon as a significant fraction of deuterium is injected into the plasma. Deuterium plasmas will sufficiently activate the machine to limit human access, so there is no advantage in having a long duration D phase before going to DT from the point of view of plant commissioning. Thus, a rapid transition from D to DT is assumed.

There are three primary scenarios envisioned for the DT operation: ELMy H-mode with a plasma gain of 10 ($Q = 10$), Hybrid scenario (characterized by $q > 1$), and an Advanced scenario aiming at long pulse, high non-inductive current drive fraction. These scenarios are briefly characterized in Table III, which include typical plasma pulse lengths, number of pulses, and envisioned NTM activity.

The EC system will be fully commissioned prior to the DT operation. This includes commissioning of all hardware systems, as well as of the control system and its algorithms for EC H&CD applications. Section III aims at describing the various functions H&CD functions allocated to the EC system based on the different plasma scenarios.

III. EC H&CD APPLICATIONS

The partitioning of the H&CD functions to the EC system has been based on the unique features of the Electron Cyclotron interaction with the plasma. The microwave beam propagates through the plasma in a collimated beam, which resembles free space Gaussian beam propagation. Note that this is characteristic of the ITER EC system where the frequency is far from cut-off densities. The power is then deposited in a relatively narrow location at the resonance, with the size depending on the beam width, plasma parameters, and launch geometry (poloidal and toroidal angles).

Typically, the deposition width is relatively small varying between 2% and 20% of the normalized plasma cross section (size determined primarily by the launcher beam optics). The deposition location can be controlled via steering mirrors

TABLE III. List and description of plasma pulse types assumed for the DT operating phase. A total of 30 000 pulses are assumed.

Scenario	I_P and B_T	Mode	q_{min}	τ_{plasma} (flat top) (s)	No. of Pulses	NTMs
Q = 10	100%	H-mode	≤1	400	20 000	q = 3/2, 2
Hybrid	12MA/100%	H-mode	>1	1000	8000	q = 2
Advanced	9MA/100%	H-mode	>2	3600	2000	None

positioned behind the blanket shield module. Thus, EC offers to ITER a unique pin-point heating (ECH) and current drive (ECCD) source that is controlled from external actuators far from the plasma. Over the past decade, the EC system design has been improved with an iterative process, aiming at achieving a balance between plasma H&CD capabilities, sound engineering design, reliability, and redundancy. This process has at times challenged the technological limits of the EC subsystems and at other times limited the functional capabilities of EC system. The remaining part of this paper aims at trying to summarize the end result of this process.

The first step of this process has been to list out the H&CD applications that can be addressed by the EC system, prioritize these applications and then allocate the applications to either the upper or equatorial launchers. Note that ITER has the two launching systems with one launcher in the equatorial (EL) port[8,9] for accessing the plasma core (on-axis to mid radius) and four in the upper (UL) ports[10,11] for accessing the outer half of the plasma. The design of these launchers depends on the allocated H&CD applications, which then determine the launchers access range, power handling, beam focusing, etc.

A. Selection of H&CD applications

The list of possible EC H&CD applications is provided in Table IV and based on past and on-going experience on magnetic fusion devices. The applications are divided into the three operating scenarios of the non-activation phase and the three scenarios of the DT activated phase. The table also identifies those applications that are driving the design. Blank entries imply that the particular plasma scenario does not necessitate a given application, for example, there is no need for sawtooth control in a Hybrid scenario as there is no $q = 1$ surface or the size is insignificant. Each application has been prioritized according to one of four categories:

TID: Applications that are **T**argeted and **I**mpact the **D**esign of the EC system.
TND: Applications that are Targeted but do Not impact the Design, as either the application is a lower priority, or can be achieved by the flexibility inherent in the design to achieve the TID applications.
NI: Applications **N**ot **I**ncluded in the list of allocated EC applications as the EC system is not efficient in achieving this application, would impact the design limiting the TID applications, or imposes too high risk to other systems.
TBA: Applications **T**o **B**e **A**ssessed, the applicability of the EC has not yet been assessed; after assessment, the application will be either "TND" or "NI."

The evaluation is based on the uniqueness of EC to provide a given function (relative to other systems available on ITER) and based on achieving the primary goals of ITER (the three D-T scenarios). ITER differs significantly from other tokamaks in that ITER will have limited scope for "quick" hardware modifications for specific experimental campaign. The in-vessel components of the EC launchers are therefore designed for the lifetime of ITER, without intervening revisions or upgrades.

There are 13 applications that have been targeted for the ITER EC system, of which 8 impact the design (TID). A brief description of how EC is envisioned to achieve each of these applications is described in Subsection III B along with a brief description how the given function has impacted the design of the EC system (see Sec. IV).

TABLE IV. The applicable EC functions for the various operating scenarios of ITER, categorized based on those applications targeted and impacting the EC system design (TID), targeted but not impacting design (TND), or those not included (NI) as targeted applications. Some applications call for further assessment (TBA or "to be assessed") to ensure the EC system is applicable.

	Non-activated				D-T		
	L-mode (half field)	H-mode (half field)	L-mode (full field)	H-mode (full field)	Q = 10	Hybrid	Advanced
Pulse duration [s]	300	300	300	50	400	1000	3600
Break down	TID	TID	TID	TID	TID	TID	TID
Burnthrough	TID	TID	TID	TID	TID	TID	TID
Elongation assist	TND	TND	TND	TND	TND	TND	TND
Current ramp-up	TND	TND	TND	TND	TND	TND	TND
Central heating	TID	TID	TID	TID	TID	TID	TID
L to H-mode assist		TND		TND	TND	TND	TND
Current profile tailoring						TID	TID
Sawtooth control	TID	TID	TID	TID	TID		
q = 3/2 NTM control		TID		TID	TID		
q = 2 NTM control		TID		TID	TID	TID	
q ≥ 5/2 NTM control		TBA		TBA	TBA	TBA	TBA
FIR control		TBA	TBA	TBA	TBA	TBA	TBA
Disruption mitigation	TBA	TBA	TBA	TBA	TBA	TBA	TBA
Diagnostic application	TBA	TBA	TBA	TBA	TBA	TBA	TBA
Impurity control		TID	TID	TID	TID	TID	TID
ELM control		NI	NI	NI	NI	NI	NI
H to L-mode assist		TND		TND	TND	TND	TND
Ramp-down assist	TND	TND	TND	TND	TND	TND	TND
Wall conditioning	NI	NI	NI	NI	NI	NI	NI

B. Functional description

The targeted EC H&CD applications are grouped according to the four periods of a plasma discharge: plasma initiation, ramp-up, flat-top, and ramp-down. Note that this is not an ideal grouping as some applications occur in multiple periods, for example, NTM control and current profile tailoring. In such an event, a given application is grouped in the period that has prescribed the design parameters of the EC subsystem(s). The plasma ramp-up and ramp-down have not been sufficiently assessed relative to the flat-top on impact to the EC system. The flat-top has been assumed the design-driver, determining the steering range and toroidal injection angles of all launchers. Therefore, the ramp-up and ramp-down are treated in the scope of this paper as equivalent, even though it is known the plasma needs different functionalities from the EC system during ramp-up than ramp-down. The control of the plasma ramp-up and down will have to adjust to the limitations of the steering range and injected power as defined in the present EC system design.

C. Plasma initiation

The EC system is to be used for plasma initiation in every discharge. The EC plays two roles: breakdown and burnthrough.

1. Breakdown

The primary functions of EC breakdown include

- inject up to 6.7 MW (8 gyrotrons) to ionize background gas, pulse lengths of $\leq$1 s, which will minimize consumption of the central solenoid Volt-seconds;
- provide breakdown over range from half (2.65 T) to full (5.3 T) field, with either the 1st or 2nd harmonic resonance layer inside the torus cross section.[12]

The main implications for the EC plant include

- adapt polarization as needed for X2 or O1 injection;
- choice of frequency compatible with resonant surface of either the first or second harmonic is found inside the plasma cross section.

The 2001 baseline design included 3 gyrotrons operating near 120 GHz and used specifically for the plasma breakdown. The ITER design review of 2007 proposed to remove the three 120 GHz gyrotrons as the 170 GHz system alone could achieve the above functionality. Removal of the 3 startup gyrotrons has been implemented in 2008–2009, and has simplified the EC plant (single operating frequency of 24 gyrotrons, rather than two operating frequencies of 27 gyrotrons). This has reduced the overall EC system, building, and service costs.

2. Burnthrough

The EC system provides additional heating following the breakdown, ensures that the plasma does not collapse due to high level of radiated power relative to the ohmic power. The main usage of the EC system during breakdown includes

- inject up to 6.7 MW (8 gyrotrons) to heat plasma, pulse lengths of $\leq$5 s;
- ensure reflection off of central column for O1 to X1 conversion (improved coupling for second pass absorption);
- deposition inside mid radius of plasma cross section over the ranges of 2.65 T to $\sim$3.2 T (X2) and $\sim$4.0 T to 5.3 T (O1).

The main implications for the EC plant include

- adapt polarization as needed for X2 or O1 injection;
- toroidal injection angle limited $\leq 25^\circ$ to ensure first pass beam incident central column to benefit from 2nd pass X1 absorption upon reflection;
- access to null region from first and/or second pass.

Note that the burnthrough application is more stringent than that for breakdown. The plasma initiation phase presents increased risk to the in-vessel components, as the pulse length is longer (increase injected power and energy), while having low first pass absorption. The low first pass absorption implies that some of the EC power will be absorbed in the plasma, with the majority of the beam power passing through the plasma and incident on the central column with $\sim$0.5% absorption (depending on incident angle and surface roughness). The resulting peak power density of the beams is $\sim$2.0 MW/m^2. Note that the blanket front wall panels are designed for a steady state load of 5.0 MW/m^2.

The microwave power will be absorbed in each subsequent passage through the plasma and each reflection off the blanket front wall panel. If the microwave power passes through the gaps between blankets, then there is a potential threat to ceramic insulators and diagnostics (such as ECE, reflectometers, or diagnostic windows). Each diagnostic system has its own mitigation system to avoid damage from the stray power during plasma initiation.

The stray power to the blanket and diagnostics is mitigated by achieving a higher second pass absorption by relying upon O1 to X1 polarization rotation upon reflection from the central column after the first pass through the plasma. X1 from the HFS (High Field Side) offers higher single pass absorption through the plasma. This imposes a toroidal limitation of the beams to $<25^\circ$ in order for the EL or UL beams to hit the central column.[12] The second pass X1 absorption increases with the toroidal angle, while for X2 the second pass absorption should be near perpendicular to the magnetic field lines for optimum absorption.

Note that toroidal angles larger than 25° are avoided for breakdown and burnthrough, as the beams will effectively miss the central column bounce around the exterior of the torus chamber. This will increase stray power in the diagnostic port plugs, increasing the risk of damaging the diagnostic instrumentation.

The burnthrough phase terminates once the radiated power in the impurities drops or burns through. At this point, the injected EC power is lowered until the X-point formation to avoid overheating the blanket wall.

D. Ramp-up

The plasma evolves through three states during the ramp-up phase. The first state is a limiter plasma (the blanket

limiting the plasma boundary), which has no applied heating power to avoid over-heating of the blankets. Then, the plasma evolves to a diverted configuration with a magnetic X-point below and the power "diverted" away from the blankets to the diverter. Once the X-point is formed, EC heating can be fully applied as the power is directed away from the blankets to the divertor, note that the diverted phase starts in L-mode and then transitions to H-mode.

The main usage foreseen of the EC system during ramp-up is to

- provide central heating and bulk current drive ($\rho_{dep} \leq 0.5$);
- provide current profile tailoring ranging from co to counter ECCD ($\rho_{dep} \leq 0.3$) and off axis co-ECCD ($0.4 \leq \rho_{dep} \leq 0.6$);
- provide control of the sawteeth ($0.4 \leq \rho_{dep} < 0.8$);
- provide NTM control ($0.6 \leq \rho_{dep} < 0.9$);

where ρ_{dep} corresponds to the EC deposition location in normalized radius. The implications for the above are enveloped with the design implications on the EC system during the flat-top.

The above deposition range provides sufficient flexibility in assisting the growth of the plasma volume current and temperature. In addition, this access range provides the ability to control the plasma current profile to avoid peaking of the central current or tailor the profile for formation of advanced scenarios or avoiding rational q-surfaces (such as the $q = 1$ for hybrid scenarios).

In order to transit from the L to H-mode, sufficient power has to be deposited within the pedestal (assumed $\rho_{dep} \leq \sim 0.8$) to exceed the H-mode power threshold. Once the H-mode is formed, the EC system will continue to provide central heating as well as control of MHD instabilities (to be discussed in Sec. III E).

During the initial operating phase of ITER, the magnetic field will be step-wise increased from half field to full field in order to extrapolate on the H-mode power threshold at full field. This threshold is estimated at 70 MW ± 50% (Ref. 7) based on multi-machine scaling. Assessing the threshold during the non-activated phase and at half field will allow a better estimate of the power needed at full field (and initiate fast track power upgrades if necessary). Scanning the magnetic field has a significant impact on the EC deposition accessibility, as the 2nd harmonic resonant location moves outward, preventing central access as above. The achievable magnetic field operating range of the EC system with X2 injection is $2.7\,T \leq B_T < 3.3\,T$.[4] This should provide sufficient measurements for scaling the power threshold to 5.3 T, which can only be achieved in the activated phase. Note that the L to H mode transition power is lower for the DT plasmas as compared to that of H or He plasmas.

E. Flattop

The most demanding phase on the EC system is the flat-top, in which multiple events will force management of the EC injected power, allocating the available 20 MW to various H&CD applications. This challenge will be most evident during half field (with He) and full field operation (with D), where there will be no additional alpha particle heating. The majority of the auxiliary heating will be needed for central plasma heating to generate and maintain a high performance H-mode. Fortunately, a majority of the H&CD applications need such a deposition inside the $q = 1$ surface with the exception of NTM control. Subsection III E 1–III E 6 briefly describes how the EC system can be used for the H&CD application in question and the desired conditions for injecting the EC power.

1. Central heating

Central heating assumes the power is deposited inside mid radius ($\rho \leq 0.5$), which is taken as a proxy for being inside the sawtooth mixing radius. A distinction is made between central heating and central current drive, in that "heating" does not directly generate current, which can be achieved by either

(a) injecting the microwaves beam perpendicular to the magnetic field;
(b) providing a balanced injection between co and counter ECCD contributions such that no net current is driven.

The main implications for the EC plant include

- Decouple the heating function from the current drive by either balancing co-ECCD and counter-ECCD contributions or inject beam perpendicular to the magnetic field surface (note that with the choice of 170 GHz, the former is chosen as the Doppler shift provides access inside $\rho \leq 0.2$ from EL.
- Adapt polarization as needed for co-ECCD, counter-ECCD or perpendicular injection.

Central "heating" can be preferable over central current drive in advanced and hybrid scenarios, which is characterized by a flat or hollow current profile. Injecting central co-ECCD is therefore detrimental for profile control for these scenarios, resulting in a peaking of the plasma current profile and destroying or degrading either the Hybrid or Advanced scenario.

An assessment was performed based on optimizing functionality and minimizing engineering challenges, which concluded that an optimized EL should provide a power fraction of 2/3 co and 1/3 counter ECCD injection.[13] The majority of H&CD applications use co injection from the equatorial plane with a toroidal angle of $\beta \sim 20°$. This toroidal injection provides a maximum driven current at mid radius. Steering the beams from perpendicular injection ($\beta \sim 0°$) to the $\beta \sim 20°$ would force a larger opening in the blanket shield module as compared to the balanced co and counter injection. The large opening has two consequences: (1) increases the thermal load on the mirrors from a larger viewing of the plasma core and (2) increases the neutron streaming through the launcher body due to a reduced labyrinth formed between the blanket opening and internal optical path. The balanced co and counter injection had the additional advantage of being able to decouple the driven current fraction for constant injected power varying between positive driven current through zero net current to negative

driven current.[13] In addition, the counter ECCD will be beneficial in other H&CD applications described below.

2. Current drive

Auxiliary current drive is essential for any tokamak to achieve long pulse operation. The additional driven current reduces the demand on the central solenoid, which inductively drives the current. The auxiliary (or non-inductive) current source includes the plasma bootstrap current and the current driven from the H&CD systems (primarily NB, LH, and EC). The microwaves drive current when the beams are injected with a toroidal angle. The microwave power is dissipated first to the positive current contributing electrons due to the Doppler shifted resonance toward the low field side with $\beta > 0°$. These electrons increase their perpendicular energy and leave behind a "hole" in the velocity space as illustrated in Figure 1. The lower energy electrons will equilibrate faster than the more energetic electrons, resulting in counter going electrons repopulating the hole on the co current side, resulting in a net increase in the toroidal plasma current.

The driven current fraction is dependent on the local electron temperature (T_e) and density (n_e), with the dependence roughly proportional to (T_e/n_e). In H-mode with flat n_e profiles and centrally peaked T_e, the EC driven current efficiency drops off rapidly outside of $\rho \sim 0.3$.[4] Typical current drive efficiencies range from 30 kA/MW (15 MA scenario) to 50 kA/MW (9 MA scenario); however, this is significantly less than the NB driven current drive efficiency of 65 kA/MW (9 MA scenario).[1]

The main implications for the EC plant include

- Inject beams with a relatively large toroidal injection angle ($\beta > 20°$).
- Steering range accessing $\rho \leq 0.5$, which is achieved by launching beams near the equatorial plane.

3. Control j(ρ)

The strength of the EC system is the localized deposition, which is controlled via external actuators (steering mirrors). Although the EC system only partially contributes to the net driven current, it is more effective in shaping the plasma current density profile, j(ρ), by maintaining a narrow EC deposition profile ($\Delta\rho \sim 0.2$), but shifting the deposition from on axis (for peaked j(ρ)) to mid radius (generating a flat or hollow j(ρ)). The largest control in j(ρ) is achieved by varying the co-and counter fractions.[14] As mentioned previously, the primary objective is to disassociate the heating function from current drive, which allows central heating (for impurity control) without effecting j(ρ), in particular, for the Hybrid and Advanced scenarios. In addition, the power fraction of 1/3 counter and 2/3 co provides sufficient flexibility in forming a monotonically increasing magnetic shear profile (all power in distributed co ECCD) to a strong reverse shear using central counter and off-axis co ECCD.

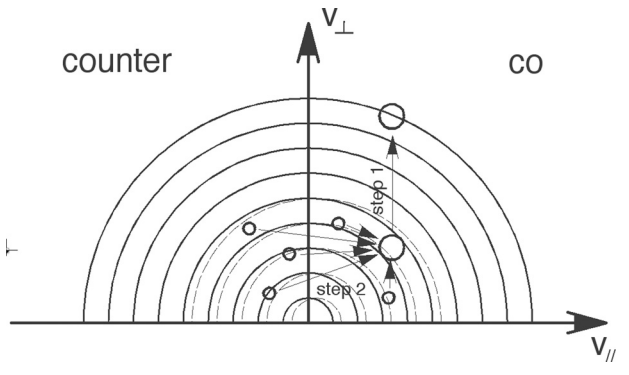

FIG. 1. EC drives current by increasing the "co" population of electrons in a two step process. Step 1: the microwaves increase the perpendicular energy of "co" going electrons, leaving a hole in the lower energetic velocity space. Step 2: the lower energetic electrons equilibrate faster, resulting in "counter" electrons redistributing to the "co" side, increasing the net "co" going population of electrons (illustrated by dashed contours).

As ITER is to be operating in scenarios ranging from centrally peaked j(ρ) (15 MA ELMy H-mode) to a reversed shear (9 MA Advanced), the launching system should have the capability of injecting 1/3 of the power in counter centrally, to full power in co ECCD distributed over $\rho < 0.5$.

The main implications for the EC plant include

- Provide co-ECCD access in the range of $0.4 \leq \rho \leq 0.6$ from all launchers.
- EL co-ECCD toroidal injection of $\beta \approx 25°$ for maximum current drive in the above range.
- Deposition width of equatorial beams of $\Delta\rho \approx 0.2$.
- Injection 1/3 of EL beams in counter-ECCD ensuring access over range of $0.1 \leq \rho \leq 0.4$.

4. Impurity Control

ITER will start with a tungsten divertor, which could result in a source of tungsten impurities that accumulate in the plasma. A mechanism to promote the transport of tungsten out of the plasma core is desired to maintain low W concentration in the plasma ($<10^{-5}$). Depositing the EC power inside of $\rho < 0.2$ has been shown to be an effective method to pump-out impurities such as tungsten,[15] and as a result the EC system has been designed to provide central heating as a potential actuator for impurity control The effect is independent of toroidal injection angle; either heating or current drive is effective provided very central deposition. However, driving current centrally will be detrimental for Hybrid and Advanced scenarios. The EC system therefore needs to be able to disassociate heating with driven current when providing core impurity control for the three desired plasma scenarios.

The impact on the EC system is equivalent to central heating.

5. Sawtooth Control

EC H&CD is an effective tool for controlling the sawtooth period, which in turn can trigger NTMs. The sawtooth frequency can be modified by changing the shear at the q = 1 surface (s_1).[16] If s_1 reaches the critical shear (s_{crit}), the sawtooth crash will occur. This can be delayed by driving co ECCD just outside the surface, which flattens the local shear, delaying the moment when $s_1 = s_{crit}$, thus prolonging (or

stabilizing) the sawtooth period. Conversely, driving current inside $q = 1$ will increase the local shear speeding up the process so that $s_1 = s_{crit}$, thus decreasing (or de-stabilizing) the sawtooth period. The process is inverted with counter ECCD, which is less effective as ECCD provides both current drive and local heating.[17] The local heating increases the local conductivity, which indirectly increases the local current drive. Thus, the co ECCD has the synergetic effect of driving current and increasing local conductivity via heating.

Both sawtooth stabilization and de-stabilization are feasible in ITER. Sawtooth destabilization is achieved by driving a significant amount of current inside the $q = 1$ surface. Neither the deposition width nor its exact location are critical, provided both are well inside the $q = 1$ surface. The sawtooth period can be decreased by a factor of 2 or less with the application of up to 20 MW of EC power.[14]

The main implications for the EC plant include

- sawtooth destabilization favors a maximum co-ECCD driven current inside the $q = 1$ surface ($\rho_{q=1}$), impact is equivalent to implications for current drive, and is achieved from the equatorial launcher;
- sawtooth stabilization favors a peaked and narrow current density profile, equivalent to the NTM stabilization, but just outside the $\rho_{q=1}$, which is assumed in the range of $0.4 \leq \rho < 0.8$.

Sawtooth stabilization can be useful for prolonging the sawtooth period longer than the plasma pulse length (useful when plasma pulse lengths are <100 s), or controlling the sawtooth crash to perform pre-emptive control of an NTM trigger.[18] Sawtooth stabilization favors a very peaked and narrow EC current density profile (j_{CD}) positioned just outside the $q = 1$ surface. An active feedback system is needed to follow the $q = 1$ surface, as the j_{CD} modifies the local shear resulting in a displacement of the $q = 1$ surface during the sawtooth evolution. The crash can be provoked by extending the power beyond the natural sawtooth period, then rapidly removing the EC power. Then, s_1 will relax on a local current redistribution time scale until $s_1 = s_{crit}$. The EC power can then be shifted to either the $q = 2$ or 3/2 to pre-emptive stabilize the NTM upon the arrival sawtooth crash perturbation that would trigger the NTM.

Therefore, the sawtooth control drive two actuators, one for de-stabilization with a large source of current drive (no dependence on j_{CD} width). The second for stabilization requiring a narrow and peaked j_{CD}, which is feedback controlled.

6. NTM Control

The NTM is a magnetic island on rational q surfaces, characterized by a difference in current inside the island relative to just outside the island. This is largely due to a significant fraction of bootstrap current (j_{BS}) outside the island. The current gradient further increases the island size until an equilibrium is formed and the island reaches a saturated width. The NTM can be stabilized by driving current inside the island, which compensates the lack of current within the island. In order to stabilize the NTM, the EC driven current density (inside the island) should exceed by 20% the missing bootstrap current density $j_{CD} \geq 1.2 \cdot j_{BS}$.[19] Once the island reduces to a marginal size ($w_{marg} = 2$ to 4 cm Refs. 20 and 21), the island will self stabilize and disappear.

The efficient stabilization of NTMs necessitates

(a) driving as much possible current inside the island, with the EC deposition width inside wmarg;
(b) modulate the power so that the driven current is generated inside the island and not at the "X" point of the island, which destabilizes the NTM.

The efficiency depends on the local j_{BS} and the j_{CD} profile (magnitude of j_{CD} and width, w_{CD}). The above criteria ($j_{CD} \geq 1.2 \cdot j_{BS}$) is valid when $w_{CD} > w_{marg}$, and modulation of the applied EC power to deposit only inside the island. The estimated modulation frequency is ≤ 3.5 kHz.[22]

When $w_{CD} \leq w_{marg}$, an alternative criterion has been proposed,[21] which can be cast in the form[23]

$$\frac{w_{CD} j_{CD}}{j_{BS}} > \frac{w_{sat}}{8}, \tag{1}$$

where w_{sat} is the saturated island width (predicted to be in the range around 30 cm for $q = 2$ NTM in the standard ELMy H-mode scenario). In this case, power modulation would lead to a modest increase of the NTM stabilization efficiency as compared to cw injection. Thus, an optimized EC system for NTM stabilization would aim at $j_{CD} > j_{BS}$ and $w_{CD} < w_{marg}$, retaining the capability of modulating the EC power up to 5 kHz and provide access the range over the plasma cross section envisioned for the relevant q surfaces.[24]

The control of the NTM instability has been a top priority of the ITER EC system, as it can lead to a considerable degradation of fusion burn performance (up to 50% (Ref. 21)) and if unmitigated can lead to an increased number of plasma disruptions. The primary role of the four upper launchers is to control the NTMs. Each upper launcher has two sets of four beams (see Sec. IV A 2) arranged to extremely narrow deposition profiles and superimposed to provide a deposition profile equivalent to the marginal island width (~4 cm width). In addition, the beams are steered over the expected range in which the $q = 3/2$ and 2 magnetic flux surfaces[23] are expected to be found for the various scenarios listed in Tables II and III.

Note that as the NTMs occur in the outer half of the plasma ($0.6 \leq \rho < 0.9$), the deposited power is more rapidly transported to the edge and thus less efficient as centralized heating. There is an inherent degradation in Q, as the more power needed for NTM stabilization lowers Q and prevents that power from being used for central heating or current drive. Thus, the UL optics have been optimized to provide an extremely peaked j_{CD} for the combined beams for a minimum of injected power, typically ≤ 8 MW.[25]

There are multiple methods in applying EC power for control of the NTMs. For example, power can be applied once an NTM is detected. For ITER, this would usually imply redirecting the power from the EL to UL, by turning off the gyrotron power and deviating the beams via the TL in-line switch. This process requires 2 to 3 s, which is slow

relative to the NTM growth rate. However, this utilizes the EL for the majority of the time for optimum central heating and current drive. Pre-emptive application of ECCD on the rational q surface is also feasible, which potentially avoids the onset of the NTM, but dedicates several MW of power that cannot be used for central heating and current drive. An alternative approach is to toggle the EC power between triggering a sawtooth crash and then stabilizing the NTM by steering the power from the same steering mirror. This can be achieved in roughly 1 to 2 s. The EC system has been designed to accommodate any of the above methods.

IV. SYSTEM DESIGN

The ITER EC system[5,6] design basis has been defined aiming at achieving the widest spectrum of functional applications (listed in Table IV), but balanced against maintaining costs and complying with EC technology limits. The power (24 MW installed) and pulse length (3600 s) push present technologies with respect to existing systems. In addition, the launcher and parts of the transmission line have to conform to the nuclear and safety requirements arising from the burning plasma environment, which further limit the functional capabilities (such as the launcher steering angles).

In the design of the EC plant, many of the parameters used to control the power injection, steering speed, polarization, etc., were not known when specifying the component design specifications. Even today, extrapolation from existing machines either leaves too large of a range or has not even been performed. Without this guidance, the specifications were driven by what is achievable by existing technologies or what could be achieved with a reasonable investment of R&D funds. As will be mentioned in Sec. V, the next step is to perform time dependent modeling to evaluate if the control of the EC plant is sufficient to achieve the multiple H&CD applications set forth as targets. Note that when a given parameter has been well defined (such as the required power and modulation frequency), the specification was limited to that value to avoid increasing costs to the EC plant for functionality that is not likely to be used.

The EC system layout was configured following a modular approach, which permits applying EC power to multiple applications at a time as well as avoids a single failure rendering a large percentage of the plant non-operating. A single main high voltage power supply (HVPS) feeds two gyrotrons, each with a dedicated TL. Each TL has an in-line switch that can direct the power from a given gyrotron to either the EL or UL launchers. Switching time is <3 s. The overall layout of the system is illustrated in Figure 2, the 12 HVPS and 24 gyrotrons are located on three levels of the RF building. The 24 TL lead from the gyrotrons, through the assembly hall and into the tokamak building. The TL switches are located outside the tokamak building wall for easier maintenance access. The EC system is located on the first (L1) and second (L2) levels of the tokamak building for accessing the equatorial and upper ports, respectively. The TL passes through the gallery and into each port cell. There are secondary confinement barriers at the tokamak wall and port cell penetrations, followed by a primary confinement

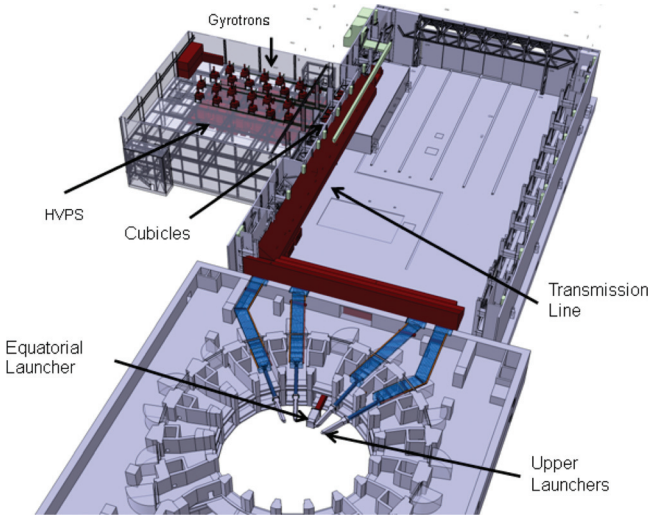

FIG. 2. Layout of the EC system with the PS and 24 gyrotrons in the RF Building (upper left) and the transmission line passing through the assembly hall to the tokamak building leading to the four upper and one equatorial launchers.

system in the port cell before leading to the launchers in the equatorial and upper ports.

Table V illustrates how the various applications described in Sec. II establish the targets on the EC system that then drive particular design aspects of the various subsystems of the EC plant.

The estimated power transmission efficiency of the plant is outlined in Table VI, starting from the 24 kV supply lines (provided by the Pulse Power Electrical network or PPEN) and leading to either the EL or UL. The total power supplied to the EC plant is $\geq$49.4 MW with an expected delivered power to the plasma of 20 MW. Each of the twenty-four 1.0 MW gyrotrons is expected to deliver 0.83 MW to the plasma. Note that the power supplies, transmission lines, and launchers are designed for a unit power of $\geq$1.5 MW, which could lead to an increase in delivered power of up to 10 MW pending gyrotron development.

The design of each of these systems and the plant control system is described in Subsections IV A–IV F, starting from the launchers and working back to the power supplies.

A. Launcher design basis

The design of the two EC launchers (EL and UL) has been driven by the partitioning of the plasma H&CD applications listed in Table IV. In general, the applications fall into two categories

(a) those requiring a narrow and peaked co ECCD deposition profile;
(b) those requiring a broad deposition profile with either co ECCD, counter ECCD, or pure heating (no net driven current).

The two categories split spatially in the plasma cross section, with Cat. (a) associated with deposition outside the plasma mid radius ($\rho \geq 0.5$) and Cat. (b) inside the plasma core ($\rho \leq 0.5$). This sets the design basis of the two launchers as illustrated in Figure 3.[2] The UL to provide a narrow and

TABLE V. A summary of the targeted applications and the associated impact on the EC system design to achieve that given function.

	Target				
	ρ_{dep}	$\Delta\rho_{dep}$	I_{CD}	j_{CD} [kA/MW]	Impact
Break down	<0.9	None	None	None	Gyrotron frequency choice
Burnthrough	<0.3	None	None	None	Gyrotron frequency and beams incident on central column for high 2nd pass absorption
Central heating, impurity control	<0.3	~0.2	~0.0 kA	0.0	Inject 1/3 power in counter to achieve heating with no net driven current
Current profile tailoring	0.4–0.6	~0.2	Maximum	None	Drives poloidal steering EL for access and maximum driven current at mid-radius, and UL access inside $\rho_{dep} = 0.5$
Sawtooth stabilization	0.4–0.6	<0.1	None	Maximum	UL access inside $\rho_{dep} = 0.4$
Sawtooth de-stabilization	<0.5	~0.2	Maximum	None	Drives poloidal steering EL for access and maximum driven current near $\rho_{dep} = 0.3$
NTM control	0.6–0.9	$\Delta\rho_{marg}$	None	$>1.3 \cdot j_{BS}$	Primary justification of ULs, optical system optimized for narrow ρ_{dep} and peaked j_{CD}

TABLE VI. The transmission efficiency along the path from plug to plasma for the EC system. Note this is assumed for a single PS coupled to two RF sources (output of 2.0 MW at gyrotron window) and along highest loss path (UL port 12). The insertion power (η_{power}) and mode (η_{mode}) transmission efficiency are provided for each component, when applicable.

Step	System	Output power (MW)	η_{power} (%)	η_{mode} (%)	Comment
1	PPEN	≥49.4	NA	NA	
2	HV PS	≥48.0	≥97	NA	Electrical efficiency of PS is rated for ≥97%
3	2 gyrotron (power at window)	≥24.0	≥50	>95	Power in TEM_{00} mode, note that this is not a critical parameter for the overall power transmission
4	2 RF source MOU	≥23.0	≥96	≥95	Power is coupled into HE_{11} mode
5	2 TL	≥20.7	≥90	>95	Mode is HE_{11}
6a	After EL	≥20.0	≥96.5	NA	Power is in primary lobe of projected beam at plasma surface
6b	After UL	≥20.0	≥96.5	NA	Power is in primary lobe of projected beam at plasma surface

peaked current density profile (deposition width ~3 to 8 cm) suited for MHD control and accessing $0.4 < \rho \leq 0.88$, while the EL to provide a broad deposition profile ($\Delta\rho \sim 0.2$) accessing $0.0 < \rho < 0.6$. In addition, the EL is to provide 1/3 of the power in counter ECCD and 2/3 in co ECCD. Pure heating is achieved by balancing the co and counter fractions at up to 2/3 of the total power.

The full 20 MW can be deposited anywhere from $\rho = 0.15$ to 0.8 with a varying degree of deposition width based on which launcher is chosen. Note that there is an overlap region ($0.4 < \rho \leq 0.6$) in which both launchers have access.

1. Equatorial launcher

The EL[8,9] groups the 24 beams in sets of 8 as illustrated in Figure 4. The beams enter the plug via a 50 mm HE_{11} corrugated waveguide, which direct the beams to a fixed mirror followed by a steering mirror. The 8 beams are steered in a vertical plane with a ~25° toroidal injection angle, which

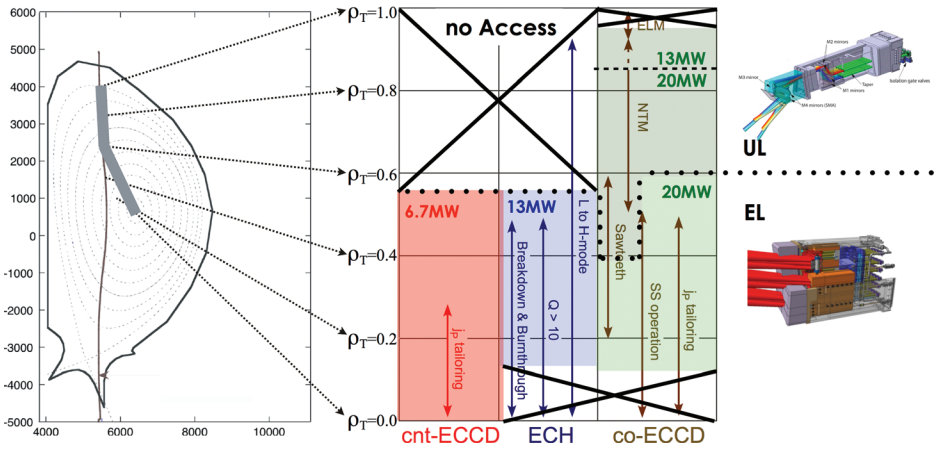

FIG. 3. The deposition access of the EL and UL across the plasma cross section and categorized based on driving counter (cnt) ECCD (shaded red), co ECCD (shaded green), or pure heating (shaded blue).

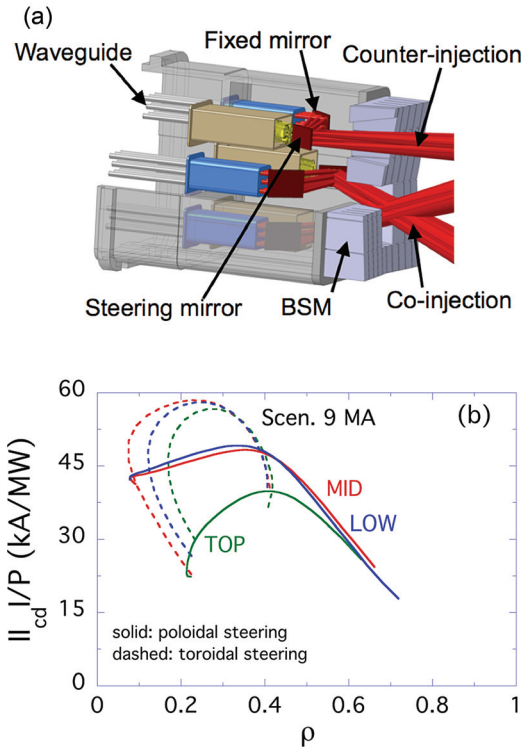

FIG. 4. (a) The equatorial launcher and (b) the resulting driven current as a function of deposition location.[12] Reprinted with permission from D. Farina *et al.*, Phys. Plasmas **21**, 061 504 (2014). Copyright 2014 American Institute of Physics.

maximizes the current drive efficiency at mid radius.[12] The two optical mirrors are configured in a horizontal plane, thus the EL has three steering rows. The top row injects the beam in the counter direction, while the middle and bottom rows in the co ECCD direction.

Prior to 2014, the EL steered the beams in a toroidal plane, which provided the largest amount of co ECCD, but limited to inside $\rho \leq 0.42$. Accessing further off axis is obtained with larger toroidal injection angles resulting in partial first pass absorption. Non-first pass absorbed power would then pass through the plasma and potentially damage other equatorial port plugs or in-vessel components. A change to poloidal steering was implemented[12,13] as it doubles the driven current at mid radius and minimizes the apertures in the EL front shield, which improves the neutron stopping potential of the launcher.

2. Upper launcher

There are four upper launchers[10,11] each with 8 entry beams split into two sets of four beams, as shown in Figure 5(a). Each beam is reflected through a four mirror optical system with the last mirror a steering mirror injecting the set of four beams in a vertical plane with a ∼20° toroidal injection angle, offering the maximum driven current density for MHD control. The two steering mirrors cover a slightly different access range but both capable of injecting 3.35 MW. The lower steering mirrors (LSMs) cover a range of $0.6\rho \leq 0.88$, and the upper steering mirrors (USMs) a range of $0.4\rho \leq 0.8$.

The four beams of a given steering mirror are to have slightly different toroidal angles so that the varying launcher positions will be nearly co-incident at the deposition location in the plasma. The corresponding expected current density as a function of ρ is shown in Figure 5(b).

3. Common launcher design aspects

The EL and UL designs are being developed in collaboration between IO and the two procuring domestic agencies (DAs): Japan for the EL and Europe for the UL. This has led to a common configuration for the ex-vessel waveguide, which forms the primary confinement system as illustrated in Figure 6. A double Helicoflex seal configuration is used to connect the waveguide components, which allows a double confinement barrier and vacuum monitoring of the interspace. An isolation valve and diamond window separate the torus vacuum from the TL vacuum. The window-valve assembly is configured to allow *in situ* leak testing (or replacement) of the window without impacting torus vacuum. The assembly is located in the port cell (outside of the bio-shield) to limit worker radiation exposure during maintenance.

A common SM design is being utilized for both the EL and UL. The SM utilizes a frictionless design[26] that can sweep the steering range in <3 s. The frictionless system also avoids backlash, offering an accurate control of the steering injection angle with corrections in angle occurring in <100 ms. The SM features a pneumatic actuator consisting of pressurized bellows and spring to control the mirror rotation. This design avoids bearings and push-pull rods that have encountered failure in conventional launcher systems. The bearings are replaced with flexure pivots providing mirror rotations up to 16° (corresponding to a beam rotation of 32°); and the push-pull rods replaced with a pneumatic actuator consisting of a piston acting against a spring. The failure modes encountered in the prototypes steering mirror assemblies are cyclic fatigue of either the spring or bellows. Improvements on both components have achieved $\geq 4 \times 10^6$ million full steering cycles with no failure. The steering mirrors are expected to undergo ∼60 000 rotations cycles of

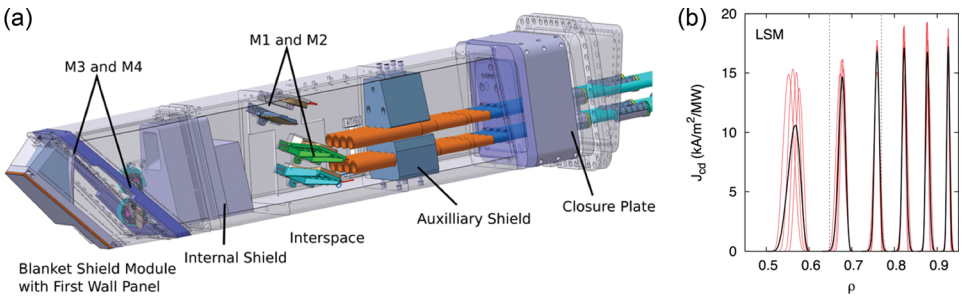

FIG. 5. (a) The upper launcher and (b) current density profiles of the 4 superimposed beams from the lower steering mirror for an optimized optical system.[34] Reprinted with permission from A. Moro *et al.*, AIP Conf. Proc. **1580**, 553 (2014). Copyright 2014 American Institute of Physics.

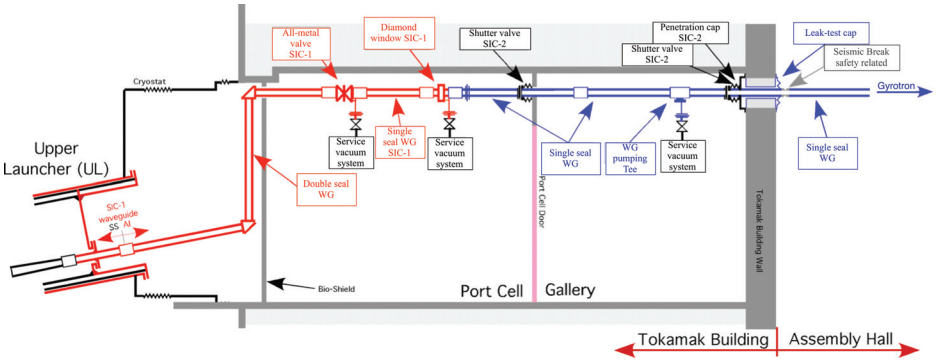

FIG. 6. The confinement system of the EC system is formed by a first confinement (red) of the HE_{11} waveguide (with double Helicoflex seals), isolation valve and diamond windows and the second confinement by shutter valves located at the port cell and tokamak walls (black).

$\sim 12^\circ$ for the plasma discharges listed in Tables II and III. These cycles typically correspond to setting of a given steering mirror from a shot to shot basis, and management of the applied power to minimize large rotations. Note that small rotations (tracking NTMs or $q = 1$ surface) do not significantly provoke cyclic fatigue.

Helium will be used for pressurizing the bellows, which offers a rapid control of the applied pressure from the servo-valve to the steering mechanism (6 to 8 m path). Note that the pressure response of the circuit is drastically changed in the event of a bellows micro-leak, in which case the circuit will be isolated and evacuated to avoid degradation of the torus pressure.

B. Transmission line

The TL[27,28] uses 63.5 mm HE_{11} waveguide to transmit the microwaves from the gyrotron to the launchers. The length is ~ 160 m and there are between 6 and 9 miter bend (or switch) reflections. The TL includes monitors of the forward going power (not calibrated), universal polarizers (two mirror configuration for controlling both the ellipticity and rotation of the major elliptical axis for optimum plasma coupling), in-line switches (to deviate the power to either the EL or the four ULs), and a switch-load (for gyrotron conditioning, see below). The switching between launchers is achieved (≤ 3 s) by shutting off the applied voltage to the gyrotrons, displacing the mechanical switch, then re-applying the voltage to the gyrotron. A "typical" transmission line is illustrated in Figure 7. The routing of the TL through the three buildings was chosen to minimize the number of mitre bends, avoiding unnecessary losses. The estimated transmission efficiency is $\geq 90\%$. This is comparable to the transmission efficiency of $\sim 95\%$ demonstrated in the JAEA TL test stand.[29] The TL includes a second switch attached to a load for gyrotron conditioning during installation, before tokamak operation and recovery after gyrotron internal breakdown (load used only between plasma pulses).

The universal polarizers will actively control each beam polarization for ideal coupling into the plasma (either O1 for nominal field or X2 for half field operation). The polarization can be swept through the entire possible ranges within 2 s, and is expected to have $\geq 98\%$ control on polarization (in electric field). Note that the largest source of error in optimizing the polarization will be the accurate knowledge of the magnetic field geometry of the last closed flux surface. The design target for control of the polarization relative to estimated magnetic field lines is $>97\%$ coupled power to the O1 (or X2 for half-field operation).

The control of the polarization is of particular concern during O1 operation, as the small percentage of X1 will be strongly refracted through the plasma resulting in ~ 25 kW per beam incident on the plasma facing components. Even components hidden behind the blankets may receive a significant portion of the refracted power as the gaps between blankets are far from cutoff.

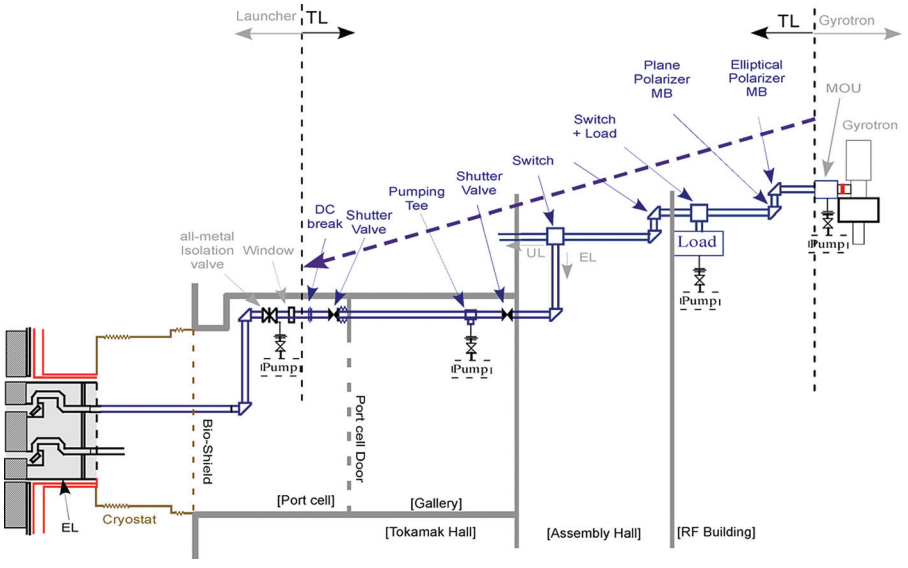

FIG. 7. A typical TL includes: power monitor, polarizers, switch-load, and switch-launchers.

C. Gyrotrons

The gyrotrons will have output powers $\geq$1 MW and operate at 170 GHz and to be supplied by four DAs. Two DAs (Russia and Japan) are advancing the output power and pulse lengths with reliable operation of $\geq$1.0 MW and $\geq$800 s already demonstrated. The present configuration assumes 16 diode and 8 triode tubes will be supplied by the four DAs. The gyrotron output power will exit a diamond window in a TEM_{00} mode that efficiently couples to TL's HE_{11} corrugated waveguide (63.5 mm). A matching optics unit (MOU) is inserted between the gyrotron and TL to shape and orientate the beam for optimum coupling to the HE_{11} waveguide.

The gyrotrons will operate with the power fully on (1.0 MW) or off (0 MW), and capable of full power modulation from 0 to 5 kHz. The total delivered power to the tokamak can be controlled in incremental steps by adding (or removing) gyrotrons. Note that operation at intermediate powers is not foreseen as it will not be relevant for a large plasma such as that of ITER. Also, operating between full and reduced power will increase the thermal loading on the gyrotron collector. The EC system operation is configured to minimize fatigue on all gyrotrons, while maintaining reasonable functional capabilities for H&CD applications. The gyrotron technology has significantly improved over the years,[30] with recent results of >95% operating reliability at 1 MW and 1000 s operation.[31]

D. Power supplies

The HVPSs consist of 12 main, 24 body (BPS), and 8 anode (APS) power supplies. The main HVPS provides the current ($\sim$110 A) and roughly half the accelerating voltage ($\sim$55 kV) of the gyrotron's electron beam. The BPS (and APS) provides additional accelerating voltage ($\sim$45 kV) in a depressed collector configuration, increasing the gyrotron electrical efficiency to $\geq$50%. All HVPS (main, APS, and BPS) are to use the pulse step modulated (PSM) concept, which provides fine voltage control and offers high frequency modulation ($\leq$5 kHz). A single main HVPS and pair of BPS (and pair of APS for triode gyrotrons) feed two gyrotrons, with the possibility of remotely connecting or disconnecting a gyrotron within a few seconds.

E. Control system

The EC Plant Control (ECPC)[32,33] system provides the local control, interlocks, and monitoring of the EC hardware and interfaces with the ITER Central I&C, i.e., CODAC and the Plasma Control System (PCS). The ECPC coordinates the operation of the whole EC system, receiving requests and/or references from the PCS and providing commands to the EC subsystems to implement those requests. In addition, the ECPC is capable of operating the EC system in various states simultaneously (conditioning gyrotrons, tokamak operation, maintenance mode, etc.).

The design and development of the ECPC have been divided into two main phases: the first phase includes the acceptance tests, integration of the subsystems and first plasma operation (FP) (8 MW); the second phase is for a fully integrated 24 MW system, including full implementation of the more complex algorithms for EC operation, e.g., NTM stabilization, automatic conditioning of gyrotrons, etc. The proposed I&C architecture includes a main plant controller and sub-system local controllers (for the PS, gyrotrons, TLs, and launchers).

F. Power upgrades

The EC system is envisaged to undergo four stages of delivered power capabilities. The first stage is for the FP, where an 8 MW system will be used for the initial break down and burnthrough of the first plasma. The injected power will be up to 6.7 MW and lasts for $\leq$100 ms. The system is to include 4 HVPS, 8 gyrotrons, 8 TLs, and one UL.

The second stage will be the complete 24 MW system (20 MW injected) for the first and second campaign, and includes the remaining 3 ULs and EL. The whole system will be capable of pulse lengths up to 3600 s, even though pulses of the order of $\leq$400 s will be required. The control system associated with the safety confinement components will be installed from the initial operation for final qualification and will allow direct transition to the activated phase of ITER operation.

The third phase will assume a partial upgrade in power, taking advantage of potential technology increases in gyrotron development. The HVPS are specified for higher current and voltage outputs to accommodate gyrotron tubes delivering between 1.2 and 1.4 MW (depending on gyrotron efficiency). All TL and launchers are specified for $\geq$1.5 MW transmitted power. A future replacement of the gyrotron tubes could therefore increase the injected power between 24 MW (installed 28.8 MW) and 28 MW (33.6 MW), without the need of upgrading the other EC sub-systems.

The fourth phase would be adding more HVPS-gyrotrons-TLs to increase the total injected power to 40 MW (installed 48 MW). The number of gyrotrons to achieve this power depends on the state of technology at the time when the upgrade will occur. Assuming an average source power of 1.2 MW (and assuming an upgrade as described in phase 3), an additional 16 gyrotrons are needed, which would either be housed in an extension to the RF building, or in the assembly hall. Following this strategy, the existing TL and launchers would not require any modification, only the addition of the 8 HVPS, 16 gyrotrons, and 16 TL leading up to the tokamak building. The TL switching network outside the tokamak building would be altered to redistribute the power between the 32 UL entries and 24 EL entries.

V. NEXT STEPS

The EC system and nearly all the sub-systems (Power Supplies, Gyrotrons, TL, and launchers) have passed the preliminary design phase with the exception of the control system. All sub-systems will be developed to the final design stage between 2014 and 2018, prior to their installation planned between 2017 and 2023. The H&CD functionality

requirements are now frozen and no longer impact the design development. As the EC system design heads toward design finalization, a complete assessment of the EC H&CD capabilities is being performed based on the targeted applications outlined in this paper. The assessment aims at determining the necessary applied power to achieve each of the desired functions and propose an optimized power management to achieve the greatest functionality of the EC heating system. This work has started in 2014 and will extend over the next 4 years.

ACKNOWLEDGMENTS

The authors would like to thank the numerous scientist and engineers involved in the EC system design development and procurement. This includes those from the five participating Domestic Agencies (Europe, India, Japan, Russia, and United States) and the associated laboratories in each of these ITER partners. In addition, the author would like to thank Dr. Kajiwara for his contribution in optimizing the Equatorial Launcher; along with the scientists working and exploiting the EC systems on ASDEX-Upgrade, DIII-D, FTU, JT-60U, KSTAR, LHD, SST-1, TCV, Tore Supra, and W7X, in addition to the JET, ORNL, and PPPL scientists. The views and opinions expressed herein do not necessarily reflect those of the ITER Organization.

[1]F. Wagner, A. Becoulet, R. Budny, V. Erckmann, D. Farina, G. Giruzzi, Y. Kamada, A. Kaye, F. Koechl, K. Lackner, N. Marushchenko, M. Murakami, T. Oikawa, V. Parail, J. M. Park, G. Ramponi, O. Sauter, D. Stork, P. R. Thomas, Q. M. Tran, D. Ward, H. Zohm, and C. Zucca, Plasma Phys. Controlled Fusion **52**, 124044 (2010).

[2]M. A. Henderson, R. Chavan, R. Bertizzolo, D. Campbell, I. Danilov, F. Dolizy, D. Farina, K. Kleefeldt, R. Heidinger, J. D. Landis, E. Poli, G. Ramponi, G. Saibene, F. Sanchez, O. Sauter, A. Serikov, H. Shidara, P. Spaeh, H. Zohm, and C. Zucca, in *Proceedings of the 14th Joint Workshop on Electron Cyclotron Emission and Electron Cyclotron Resonance Heating, Santorini, Greece*, edited by A. Lazaros (Heliotopos Conferences Ltd., Athens, 2006), p. 558.

[3]G. Ramponi, D. Farina, M. A. Henderson, E. Poli, G. Saibene, and H. Zohm, Fusion Sci. Technol. **52**, 193–201 (2007), available at http://www.ans.org/pubs/journals/fst/a_1498.

[4]D. Farina, M. Henderson, L. Figini, G. Ramponi, and G. Saibene, Nucl. Fusion **52**, 033005 (2012).

[5]T. Omori, M. A. Henderson, F. Albajar, S. Alberti, U. Baruah, T. S. Bigelow, B. Beckett, R. Bertizzolo, T. Bonicelli, A. Bruschi, J. B. Caughman, R. Chavan, S. Cirant, A. Collazos, D. Cox, C. Darbos, M. R. de Baar, G. Denisov, D. Farina, F. Gandini, T. Gassmann, T. P. Goodman, R. Heidinger, J. P. Hogge, S. Illy, O. Jean, J. Jin, K. Kajiwara, W. Kasparek, A. Kasugai, S. Kern, N. Kobayashi, H. Kumric, J. D. Landis, A. Moro, C. Nazare, Y. Oda, I. Pagonakis, B. Piosczyk, P. Platania, B. Plaum, E. Poli, L. Porte, D. Purohit, G. Ramponi, S. L. Rao, D. A. Rasmussen, D. M. S. Ronden, T. Rzesnicki, G. Saibene, K. Sakamoto, F. Sanchez, T. Scherer, M. A. Shapiro, C. Sozzi, P. Spaeh, D. Strauss, O. Sauter, K. Takahashi, R. J. Temkin, M. Thumm, M. Q. Tran, V. S. Udintsev, and H. Zohm, Fusion Eng. Des. **86**, 951 (2011).

[6]M. A. Henderson and G. Saibene, Nucl. Fusion **48**, 054017 (2008).

[7]D. J. Campbell and ITER Collaborators, "Challenges in burning plasma physics: The ITER research plan," in *Proceedings of the 24th International Conference on Fusion Energy, San Diego, USA, 2012* (IAEA, Vienna, 2012), ITR/P1-18.

[8]K. Takahashi, K. Kajiwara, N. Kobayashi, A. Kasugai, and K. Sakamoto, Nucl. Fusion **48**, 054014 (2008).

[9]K. Takahashi, Y. Oda, K. Kajiwara, N. Kobayashi, M. Isozaki, K. Sakamoto, T. Omori, and M. Henderson, in *Proceedings of the 20th Topical Conference on Radio Frequency Power in Plasmas* (2013), p. 546.

[10]M. A. Henderson, R. Heidinger, D. Strauss, R. Bertizzolo, A. Bruschi, R. Chavan, E. Ciattaglia, S. Cirant, A. Collazos, I. Danilov, F. Dolizy, J. Duron, D. Farina, U. Fischer, G. Gantenbein, G. Hailfinger, W. Kasparek, K. Kleefeldt, J.-D. Landis, A. Meier, A. Moro, P. Platania, B. Plaum, E. Poli, G. Ramponi, G. Saibene, F. Sanchez, O. Sauter, A. Serikov, H. Shidara, C. Sozzi, P. Spaeh, V. S. Udintsev, H. Zohm, and C. Zucca, Nucl. Fusion **48**, 054013 (2008).

[11]D. Strauss, G. Aiello, A. Bruschi, R. Chavan, D. Farina, L. Figini, M. Gagliardi, V. Garcia, T. P. Goodman, G. Grossetti, C. Heemskerk, M. A. Henderson, W. Kasparek, A. Krause, J.-D. Landis, A. Meier, A. Moro, P. Platania, B. Plaum, E. Poli, D. Ronden, G. Saibene, F. Sanchez, O. Sauter, T. Scherer, S. Schreck, A. Serikov, C. Sozzi, P. Spaeh, A. Vaccaro, and B. Weinhorst, Fusion Eng. Des. **89**, 1669–1673 (2014).

[12]D. Farina, M. A. Henderson, L. Figini, and G. Saibene, Phys. Plasmas **21**, 061504 (2014).

[13]M. A. Henderson and Collaborators from F4E with the EU Associations, JA-DA with JAEA, IN-DA, RF-DA, and USIPO, in Proceedings of the IAEA 24th Fusion Energy Conference, San Diego, USA (2012), ITR/P1-06.

[14]C. Zucca, O. Sauter, M. A. Henderson, E. Fable, D. Farina, G. Ramponi, G. Saibene, and H. Zohm, AIP Conf. Proc. **1069**, 361 (2008).

[15]R. Neu, R. Dux, A. Geier, A. Kallenbach, R. Pugno, V. Rohde, D. Bolshukhin, J. C. Fuchs, O. Gehre, O. Gruber, J. Hobirk, M. Kaufmann, K. Krieger, M. Laux, C. Maggi, H. Murmann, J. Neuhauser, F. Ryter, A. C. C. Sips, A. Stäbler, J. Stober, W. Suttrop, H. Zohm, and the ASDEX Upgrade Team, Plasma Phys. Controlled Fusion **44**, 811 (2002).

[16]I. Chapman, J. P. Graves, O. Sauter, C. Zucca, O. Asunta, R. J. Buttery, S. Coda, T. P. Goodman, V. Igochine, T. Johnson, M. Jucker, R. J. La Haye, M. Lennholm, and JET-EFDA Contributors, Nucl. Fusion **52**, 063006 (2012).

[17]M. A. Henderson, T. P. Goodman, J.-Ph. Hogge, Z. A. Pietrzyk, A. Pochelon, and O. Sauter, Fusion Eng. Des. **53**, 241 (2001).

[18]F. Felici, T. P. Goodman, O. Sauter, G. Canal, S. Coda, B. P. Duval, J. X. Rossel, and the TCV Team, Nucl. Fusion **52**, 074001 (2012).

[19]H. Zohm, G. Gantenbein, F. Leuterer, M. Maraschek, E. Poli, L. Urso, and the ASDEX Upgrade Team, Plasma Phys. Controlled Fusion **49**, B341 (2007).

[20]R. J. La Haye, R. Prater, R. J. Buttery, N. Hayashi, A. Isayama, M. E. Maraschek, L. Urso, and H. Zohm, Nucl. Fusion **46**, 451 (2006).

[21]O. Sauter, M. A. Henderson, G. Ramponi, H. Zohm, and C. Zucca, Plasma Phys. Controlled Fusion **52**, 025002 (2010).

[22]ITER Physics Expert Group on Energetic Particles, Heating and Current Drive and ITER Physics Basis Editors, Nucl. Fusion **39**, 2495 (1999).

[23]E. Poli, C. Angioni, F. J. Casson, D. Farina, L. Figini, T. P. Goodman, O. Maj, O. Sauter, H. Weber, H. Zohm, G. Saibene, and M. A. Henderson, "On the criteria guiding the design of the upper electron-cyclotron launcher for ITER," Nucl. Fusion **55**, 013024 (2015).

[24]G. Ramponi, D. Farina, M. A. Henderson, E. Poli, O. Sauter, G. Saibene, H. Zohm, and C. Zucca, Nucl. Fusion **48**, 054012 (2008).

[25]L. Figini, D. Farina, M. Henderson, A. Mariani, E. Poli, and G. Saibene, "Assessment of the ITER electron cyclotron upper launcher capabilities in view of an optimized design," Plasma Phys. Controlled Fusion (submitted).

[26]J. D. Landis *et al.*, in *Proceedings of the 22nd IEEE/NPSS Symposium on Fusion Engineering (SOFE07), Albuquerque, New Mexico, USA, 2007*.

[27]F. Gandini, T. S. Bigelow, B. Becket, J. B. Caughman, D. Cox, C. Darbos, T. Gassmann, M. A. Henderson, O. Jean, K. Kajiwara, N. Kobayashi, C. Nazare, Y. Oda, T. Omori, D. Purohit, D. A. Rasmussen, D. M. S. Ronden, G. Saibene, K. Sakamoto, M. A. Shipiro, K. Takahashi, and R. J. Temkin, Fusion Sci. Technol. **59**, 709 (2011).

[28]M. A. Shapiro, E. J. Kowalski, J. R. Sirigiri, D. S. Tax, R. J. Temkin, T. S. Bigelow, J. B. Caughman, and D. A. Rasmussen, Fusion Sci. Technol. **57**, 196 (2010), available at http://www.ans.org/store/j_9467.

[29]K. Takahashi, K. Kajiwara, Y. Oda, A. Kasugai, N. Kobayashi, K. Sakamoto, J. Doane, R. Olstad, and M. Henderson, Rev. Sci. Instrum. **82**, 063506 (2011).

[30]K. Kajiwara, A. Kasugai, Y. Oda, K. Takahashi, K. Sakamoto, C. Darbos, and M. Henderson, J. Infrared, Millimeter, Terahertz Waves **32**, 329–336 (2011).

[31]A. Krasilnikov, in *Proceedings of the IAEA 25th Fusion Energy Conference, St. Petersburgh, Russia, 2014, OV/2-1*.

[32]D. Purohit, D. Billava, M. Cavinato, C. Darbos, F. Gandini, T. Gassman, G. Granucci, M. A. Henderson, T. Omori, Y. Oda, G. Sabienne, F. Sartori, and C. Sozzi, in *Proceedings of the 18th Joint Workshop on Electron*

Cyclotron Emission and Electron Cyclotron Resonance Heating, Nara, Japan, 2014.
[33]F. Albajar, T. Bonicelli, G. Carannante, M. Cavinato, F. Cismondi, C. Darbos, P. Dharmesh, M. Gagliardi, F. Gandini, T. Gassmann, M. Henderson, R. Nousiainen, G. Saibene, F. Sartori, K. Takahashi, and the EU Team, in *Proceedings of the 18th Joint Workshop on Electron Cyclotron Emission and Electron Cyclotron Resonance Heating, Nara, Japan, 2014*.
[34]A. Moro, A. Bruschi, L. Figini, R. Chavan, D. Farina, T. P. Goodman, A. Krause, M. A. Henderson, J. D. Landis, P. Platania, G. Saibene, F. Sanchez Galan, C. Sozzi, and M. Toussaint, AIP Conf. Proc. **1580**, 550 (2014).